Comparative Medicine
Copyright 2022
by the American Association for Laboratory Animal Science

Vol 72, No 2
April 2022
Pages 93–103

Original Research

Effects of Exogenous ATP on Melanoma Growth and Tumor Metabolism in C57BL/6 Mice

Yali Lei,[†] Xu Zhou,[†] Yang Zhao, and Jianfa Zhang[*]

Altered energy metabolism (glucose, lipid, amino acid) is a hallmark of cancer growth that provides the theoretical basis for the development of metabolic therapies as cancer treatments. ATP is one of the major biochemical constituents of the tumor microenvironment. ATP promotes tumor progression or suppression depending on various factors, including concentration and tumor type. Here we evaluated the antitumor effect of extracellular ATP on melanoma and the potential underlying mechanisms. A subcutaneous tumor model in mice was used to investigate the antitumor effects of ATP. Major lymphocyte cell changes and intratumoral metabolic changes were assessed. Metabolomic analysis (^{1}H nuclear magnetic resonance spectroscopy) was performed on tumor samples. We measured the activities of lactate dehydrogenase A (LDHA) and LDHB in the excised tumors and serum and found that ATP and its metabolites affected the proliferation of and LDHA activity in B16F10 cells, a murine melanoma cell line. In addition, treatment with ATP dose-dependently reduced tumor size in melanoma-bearing mice. Moreover, flow cytometry analysis demonstrated that the antitumor effect of ATP was not achieved through changes in T-cell or B-cell subsets. Metabolomics analysis revealed that ATP treatment simultaneously reduced multiple intratumoral metabolites related to energy metabolism as well as serum and tumor LDHA activities. Furthermore, both ATP and its metabolites significantly suppressed both tumor cell proliferation and LDHA activity in the melanoma cell line. Our results in vivo and in vitro indicate that exogenous ATP inhibits melanoma growth in association with altered intratumoral metabolism.

Abbreviations: G6PDH, glucose 6-phosphate dehydrogenase; LDH, lactate dehydrogenase; NMR, nuclear magnetic resonance

DOI: 10.30802/AALAS-CM-21-000099

Melanoma is one of the most malignant and metastatic cancers, with a poor prognosis and considerable drug resistance.[24] Although several agents have received FDA approval in the past decade for the treatment of melanoma, it still accounts for 47% of skin cancer deaths in humans.[40] These therapeutics, which are based on mutant genes and immune antibodies, can have serious side effects, such as diarrhea, arthralgia, and fatigue.[29] In addition, low response rates and modest clinical benefits are prevalent weaknesses of immunotherapy.[25]

Remodeling of cellular metabolism to meet the anabolic and bioenergetic demands in a constantly changing microenvironment is a hallmark of cancer cells. Canonical alterations of metabolic pathways in tumor cells involve glycolysis, glutaminolysis, and lipid metabolism and suggest a point for therapeutic intervention.[18] For example, L-asparaginase (for amino acid asparagine depletion),[16,28] and 3-bromopyruvic acid (for glycolysis inhibition)[52] have been approved for clinical use against melanoma. However, as an efficient anticancer strategy, therapeutic targeting of various metabolic pathways has met with limited success.

Rapidly growing tumor cells also typically display altered aerobic glycolysis. LDHA, a key enzyme in tumor metabolism, catalyzes pyruvate to lactate.[13] Due to its high expression in tumors and restricted expression in normal tissues, LDHA is an attractive target for cancer therapy.[31] Several LDHA inhibitors, including gossypol,[7] FX11,[26] galloflavin,[12] N-hydroxyindole–based compounds,[15] have shown significant antitumor activity in cellular and animal models. Moreover, reducing LDHA expression can suppress tumor growth and metastasis, as reported for treatment of Ewing sarcoma, breast cancer, and colon cancer.[23,46,50]

ATP is a ubiquitous intracellular high-energy substance and an important component of the tumor microenvironment.[38,39] In past studies, extracellular ATP has been broadly investigated as a signaling molecule in several tumor models.[4,6,10,44] Specifically, ATP has been reported to induce the death of mouse glioma cells via the P2X7 receptor.[41] Because most previous studies have focused on the signal transduction pathway through which extracellular ATP induces tumor cell death,[9,48] we chose to study the antitumor effect of ATP in terms of energy metabolism.

In the present study, we investigated the therapeutic effects of extracellular ATP against melanoma and performed intratumoral metabolic profiling. In addition, we assessed the effects of ATP on melanoma proliferation and LDHA activity in vitro. We demonstrated that extracellular ATP altered glucose and amino acid metabolism in melanoma cells, causing disorders in intratumoral energy metabolism and restraining melanoma growth.

Materials and Methods

Experimental animals. C57BL/6 mice (male, 6 to 8 wk old, 20 to 22 g) were purchased from the Model Animal Research Center of Nanjing University (Nanjing, China). The mice were housed in a standard animal facility (ambient temperature, 22

Received: 10 Nov 2021. Revision requested: 22 Dec 2021. Accepted: 21 Feb 2022.
Center for Molecular Metabolism, Nanjing University of Science and Technology, Nanjing, China
[*]Corresponding author. Email: jfzhang@njust.edu.cn
[†]These authors contributed equally to this work.

to 25 °C; relative humidity, 40% to 60%; standard ventilated caging system made of polysulfone with autoclaved aspen-chip bedding; a cotton nestlet and an aspen gnawing block for environmental enrichment) under a 12:12-h light:dark cycle and were provided with standard food (Xietong Pharmaceutical Biotechnology Limited Liability Company, Jiangsu, China) and water. Mice were housed in groups of 2 to 3 per cage. Mice were maintained under SPF conditions and underwent regular pathogen monitoring by sentinel screening (performed by GemPharmatech, Jiangsu, China). All animal care and use procedures were approved by the Nanjing University of Science and Technology IACUC. Research using animals was performed according to the ARRIVE guidelines.[34]

Cell culture. The B16F10 mouse melanoma cell line (catalog no. TCM36) was purchased from the Type Culture Collection of the Chinese Academy of Sciences (Shanghai, China). Cells were cultured in RPMI1640 medium (Gibco, Waltham, MA) supplemented with 10% FBS and 1% penicillin–streptomycin (Sigma, St Louis, MO) and maintained in an incubator at 37 °C with 5% CO_2.

Establishment of melanoma-bearing model. C57BL/6 mice were divided randomly into 4 groups (n = 5 in each group). Mouse melanoma (provided as a subcutaneous injection of B16F10 cells at a dose of 2×10^5 per mouse in 100 µL PBS) was used to investigate tumor growth and drug response.[43] The 4 experimental groups are designated CK (no melanoma controls), M (model; melanoma but no ATP), LATP (melanoma and low dose ATP), and HATP (melanoma and high dose ATP). Mice in the CK group received subcutaneous injections of PBS but did not receive melanoma or ATP injections. At 24 h after the melanoma injection, mice in the M group were intraperitoneally injected with 0.9% saline (no-ATP controls); those in the LATP group were injected intraperitoneally with a low dose of ATP (1 mmol/kg body weight); and those in the HATP group were injected intraperitoneally with a high dose of ATP (2 mmol/kg body weight). ATP disodium salt hydrate (catalog no. A1852, Sigma) was dissolved in 0.9% saline and filter-sterilized before injection. Mice received daily injections of ATP (or saline) for 14 consecutive days, after which they were anesthetized by isoflurane inhalation and euthanized by cervical dislocation. Blood and tissues were collected for further analysis.

Flow cytometry. Single-cell suspensions were generated from the thymus and spleen and analyzed by flow cytometry, as previously described.[30] Briefly, the tissues were minced and gently pressed through sterilized gauze (200 mesh) to obtain a homogeneous cell suspension. RBC were lysed by using ammonium–chloride–potassium buffer. Single-cell suspensions were stained with monoclonal antibodies for CD4 (dilution 1:100; clone GK1.5, catalog no. 11-0041-82, eBioscience, San Diego, CA), CD8 (dilution 1:100; clone 53-6.7, catalog no. 45-0081-80, eBioscience), B220 (dilution 1:200; clone RA3-6B2, catalog no. 11-0452-82, eBioscience), and CD19 (dilution 1:200; clone 1D3/CD19, catalog no. 152402, Biolegend, San Diego, CA). The analysis was performed using a NovoCyte flow cytometer (ACEA Bioscience, San Francisco, CA).

Sample preparation for nuclear magnetic resonance (NMR) spectroscopy. Metabolites were extracted from tumor tissues as previously described.[2] Briefly, tumor tissues were weighed and homogenized in an acetonitrile:water solution (acetonitrile:water = 1:1 [v/v], 5 mL/g). After vortexing and centrifugation (12,000 × g, 10 min, 4 °C), the supernatants containing the extracted metabolites were transferred into new tubes, and acetonitrile was completely removed by using a nitrogen-blowing concentrator. Before ^{1}H-NMR measurement, the extracts were stored at −80 °C overnight, lyophilized in a vacuum concentrator, and dissolved in 550 µL 99.8% D_2O phosphate buffer (0.2 M, pH = 7.0) containing 0.05% (w/v) sodium 3-(trimethylsilyl) propionate-2,2,3,3-d4. After vortexing and centrifuging, the supernatants were then transferred into 5-mm NMR tubes for direct analysis.

Processing and analysis of ^{1}H-NMR data. The ^{1}H-NMR spectra of all samples were acquired on an AVANCE III 500 MHz NMR spectrometer (Bruker, Karlsruhe, Germany) at 298K. D_2O was used for field frequency locking, and sodium 3-(trimethylsilyl) propionate-2,2,3,3-d4 served as a chemical shift reference. NMR spectra were phase- and baseline-corrected (MestReC version 3.7.4, Mestrekab Research, Santiago de Compostela, Spain), converted into ASCII files, and imported into R software.[35] The water signal and affected neighboring regions between 4.5 and 5.6 ppm were discarded, and the remaining spectra were normalized and pareto-scaled to facilitate comparing samples. A supervised orthogonal partial least-squares discriminant analysis was performed for multivariate statistical analysis. Metabolites were assigned according to published data,[19,45] information in metabolism databases, and software analysis (NMR suite version 8.0, Chenomx, Edmonton, Alberta, Canada).

Cell viability. Cell viability was assessed by using the MTT assay. Briefly, B16F10 cells were seeded into 96-well plates (5×10^3 cells per well), cultured for 18 h, and then cultured in the presence of various concentrations of ATP or its metabolites for 24 h. After treatment, 50 µL of MTT solution was added to each well and incubated at 37 °C for 4 h; MTT formazan was dissolved in 150 µL DMSO. Absorbance at a wavelength of 550 nm was measured by using a microplate spectrophotometer.

Measurement of LDHA, LDHB, and glucose-6-phosphate dehydrogenase (G6PDH) activity. LDHA activity was measured as described previously.[54] Briefly, samples were added to a reaction mixture containing 200 mM Tris-HCl (pH 7.4), 1 mM sodium pyruvate, and 0.5 mM NADH. LDHA activity was monitored as the decrease in absorbance at 340 nm. LDHB activity was determined by using a kit (catalog no. A020, Nanjing Jiancheng Bioengineering Institute, Jiangsu, China) according to the manufacturer's instructions. G6PDH activity was measured by using a kit (catalog no. BC0265, Solarbio Science and Technology, Beijing, China) according to the manufacturer's protocol. Enzyme activities were normalized to protein concentrations determined by using a BCA Protein Assay Kit (catalog no. P0012, Beyotime, Jiangsu, China).

Detection of reactive oxygen species. Intracellular reactive oxygen species were measured using a Reactive Oxygen Species Assay Kit (catalog no. CA1410, Solarbio Science and Technology) according to the manufacturer's protocol.

Immunoblot analysis. Cell samples were lysed in radioimmunoprecipitation assay (RIPA) buffer. Lysates were resolved by SDS–PAGE gel electrophoresis, and proteins were blotted onto 0.22-µm nitrocellulose membranes. The membranes were blocked in 5% skim milk for 1 h at room temperature and incubated overnight with AMPK antibody (dilution 1:1,000; catalog no. 2532, Cell Signaling Technology), antiphospho-AMPK (dilution 1:1,000; catalog no. 2531S, Thr172, Cell Signaling Technology, Danvers, MA), or β-actin (dilution 1:1,000; catalog no. 20536-1AP, Proteintech, Rosemont, IL) and then for 1 h with HRP-labeled goat anti rabbit secondary antibody (dilution 1:10,000; catalog no. 111-035-003, Jackson Immuno Research, West Grove, PA). For visualization, ECL solution (WB2, Solarbio, Beijing, China) was used according to the manufacturer's instructions.

Statistical analysis. The data were analyzed by using Prism 8 software (GraphPad Software, San Diego, CA). Results are presented as mean ± 1 SD. Sample sizes were selected in accordance with the 3R principle and published data.[53,56] One-way and two-way ANOVA were used to evaluate differences between groups; differences were considered statistically significant at a P value of less than 0.05.

Results

Effect of extracellular ATP on tumor growth in melanoma-bearing mice. To evaluate the antitumor activity of ATP, we established a mouse melanoma model by subcutaneous implantation of tumor cells into the left axillary of the mice. After 2 wk of ATP treatment, tumor nodules were excised and measured. The data showed a reduction in tumor growth in ATP-treated groups, especially the HATP group (Figure 1 A). The average tumor weight (mean ± 1 SD) of the M group was 1002 ± 30 mg as compared with 506 ± 55 mg in the LATP group (P = 0.00003) and 272 ± 68 mg in the HATP group ($P = 1.2 \times 10^{-6}$) (Figure 1 B). These data indicate that extracellular ATP inhibited tumor growth in a mouse melanoma model.

Effect of extracellular ATP on T-cell and B-cell subsets. The percentages of T-cell subsets ($CD4^+$ and $CD8^+$ cells) in thymus, spleen and splenic B-cell subsets ($B220^+$ and $CD19^+$ cells) were quantified by flow cytometry in all groups (Figure 2 A). None of the subsets differed significantly between organs or among groups (Figure 2 B through H). Together, these results demonstrate that the major T and B lymphocyte subsets were not significantly affected by providing extracellular ATP.

Effect of extracellular ATP on intratumoral metabolic profiling. To investigate the metabolic changes caused by exogenous extracellular ATP, we examined the metabolic profiles of tumor tissues in the M and HATP groups. Representative ^{1}H-NMR spectra with assigned metabolites of tumor extracts are illustrated in Figure 3 A. Orthogonal partial least-squares discriminant analysis models were generated to show variation in metabolites between the 2 groups. In the score plot (Figure 3 B), the HATP group was clearly distinct from the M group, suggesting significant metabolic differences between the 2 groups. The S-plot (Figure 3 C) and corresponding color-coded loading plot (Figure 3 D and E) indicate lower levels of isoleucine (P = 0.035), lactate (P = 0.0203), arginine (P = 0.0325), isocitrate (P = 0.0246), malate (P = 0.0237), uracil (P = 0.0275), AMP (P = 0.0183), and tyrosine (P = 0.00003) and higher levels of taurine (P = 0.0107) and UDP-glucose (P = 0.0331) in the HATP group as compared with the M group. Statistical analysis of the major metabolites (Table 1) indicates that ATP treatment dampened glycolysis. However, the tumor could be using the pentose phosphate pathway to compensate for inhibition of the glycolysis pathway. Therefore, we measured the activity of glucose 6-phosphate dehydrogenase (G6PD), a rate-limiting enzyme of the pentose phosphate pathway, and found that ATP treatment also reduced G6PD enzymatic activity (Figure 4). These results indicate that ATP treatment changed intratumoral metabolites related to energy metabolic pathways.

Effects of ATP on LDHA activities in the tumor and serum. Intratumoral metabolic profiling showed a significant reduction in lactate levels (mean = 2291, SD = 198 in M group; mean = 2036, SD = 124 in HATP group; P = 0.0203). Lactate is produced by the catalysis of LDHA in the glycolysis pathway and is a metabolic biomarker for the initiation and progression of melanoma.[14,21] Therefore, we measured the LDHA and LDHB activities in excised tumors and serum. ATP treatment reduced intratumoral LDHA activity in a dose-dependent pattern, whereas LDHB activity was significantly higher (P = 0.0102) (Figure 5 A and B). Serum LDHA activity was significantly higher in the M group as compared with the CK group and was not significantly different from normal in LATP and HATP groups (Figure 5 C). Serum LDHB activity was not different among the 4 groups (Figure 5 D). These data indicate that ATP can reduce LDHA activity in tumor and serum.

Effect of ATP on B16F10 cells and LDHA activity. Extracellular ATP can be rapidly degraded to ADP, AMP, and IMP, resulting in the accumulation of adenine nucleotide metabolites, including adenosine, inosine, hypoxanthine, xanthine, and uric acid. To further understand the antitumor mechanism of ATP, we used the MTT assay to assess in vitro antitumor effects of ATP and its metabolites. Treatment with various concentrations of ATP and its metabolites for 24 h significantly reduced cell viability in a dose-dependent manner. Deaths rates of about 70% and 60% occurred when the cells were exposed to 1 mM and 1.5 mM ATP, respectively (Figure 6 A). AMP and IMP showed significant ability to kill tumor cells (AMP: P = 0.0127 for 500 μM, P = 0.00004

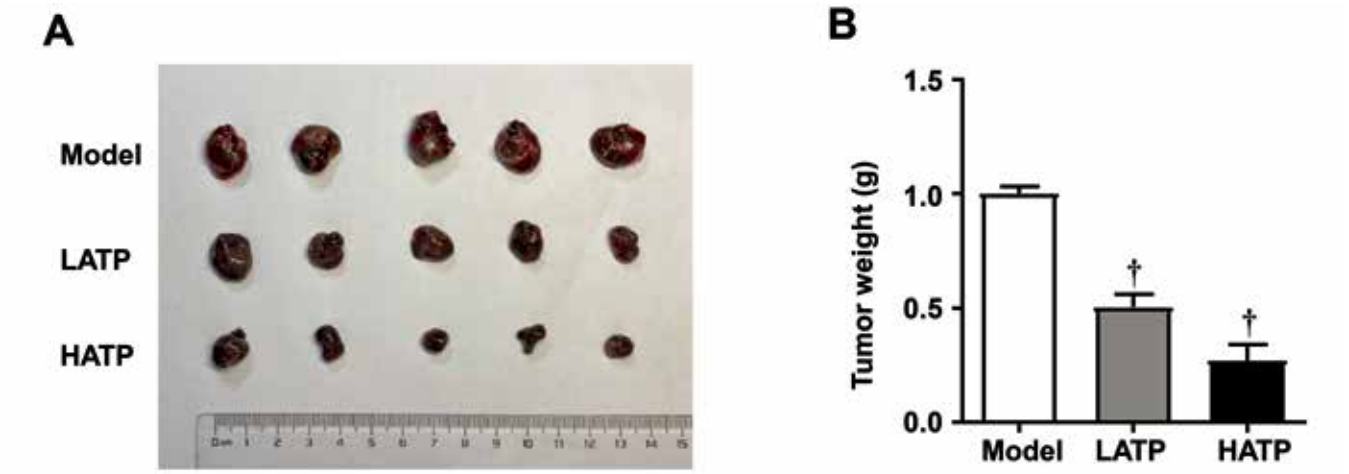

Figure 1. ATP inhibited tumor growth in melanoma-bearing mice. (A) Images of excised tumor tissues from melanoma-bearing mice. (B) Tumor weights of melanoma-bearing mice at the end of treatment; ATP (1 or 2 mmol/kg body weight) was administered starting 1 d after injection of B16F10 tumor cells. Tumor tissues of all mice were excised for measurement. Data are shown as mean ± 1 SD (n = 5). $^\dagger P < 0.01$ compared with the Model group. CK, no-melanoma controls; Model, no-treatment controls; HATP, high-dose–ATP-treated mice; LATP, low-dose–ATP-treated mice.

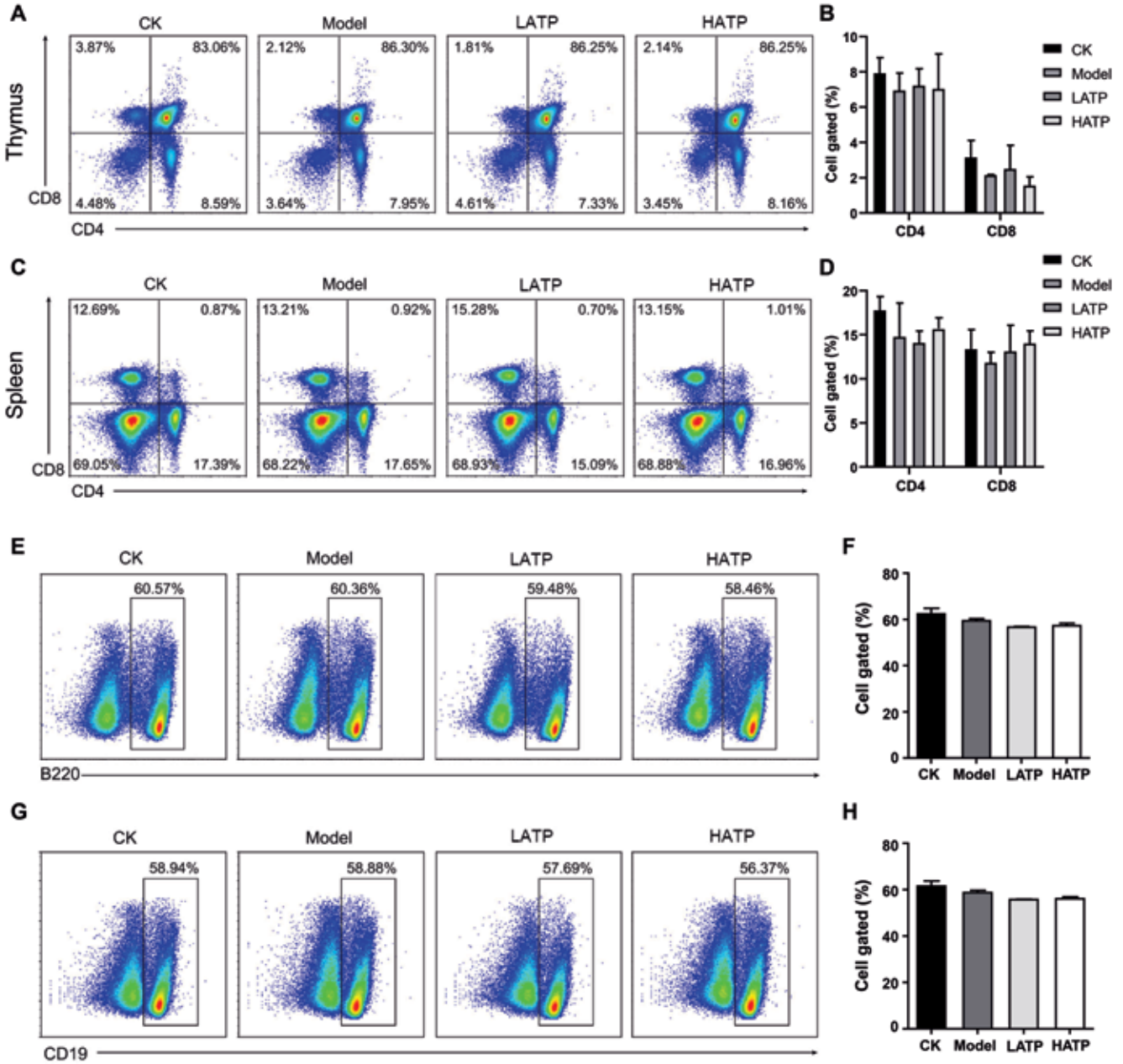

Figure 2. ATP did not affect the homeostasis of T-cell and B-cell subsets. (A) Representative flow cytometric plots and (B) flow cytometric quantification of $CD4^+$ and $CD8^+$ T-cell subsets in the thymus. (C) Representative flow cytometric plots and (D) flow cytometric quantification of $CD4^+$ and $CD8^+$ T-cell subsets in the spleen. (E) Representative flow cytometric plots and (F) flow cytometric quantification of $B220^+$ B-cell subsets in the spleen. (G) Representative flow cytometric plots and (H) flow cytometric quantification of $CD19^+$ B-cell subsets in the spleen. Data are shown as mean ± 1 SD (n = 5).

for 750 µM, $P < 0.00001$ for 1 mM, $P < 0.00001$ for 1.5 mM; IMP: $P = 0.0008$ for 500 µM, $P = 0.0002$ for 750 µM, $P = 0.0002$ for 1 mM, $P < 0.00001$ for 1.5 mM) (Figure 6 B and C).

Figure 6 D through H show the in vitro effects of adenine nucleotide metabolites on tumor cell viability. Adenosine and hypoxanthine exhibited significant cytotoxicity (Adenosine: $P = 0.0144$ for 500 µM, $P = 0.0001$ for 750 µM, $P < 0.0001$ for 1 mM, $P < 0.0001$ for 1.5 mM; Hypoxanthine: $P = 0.0019$ for 10 µM, $P < 0.0001$ for 15 µM, $P < 0.0001$ for 20 µM), whereas inosine significantly promoted proliferation ($P = 0.0357$ for 500 µM, $P < 0.0001$ for 1 mM, $P < 0.00001$ for 1.5 mM; xanthine had no significant effect on cell survival. Among all metabolites, uric acid had the most potent antitumor activity, as treatment with 750 µM and 1 mM uric acid killed about 45% and 53% of cells, respectively.

To investigate how ATP and its metabolites exerted these cytotoxic effects, we measured LDHA activity in B16F10 cells. ATP produced the greatest reduction in LDHA activity (Figure 6 I). Moreover, LDHA activity was not significantly different among cells treated with AMP, IMP, hypoxanthine, or xanthine, whereas the LDHA activity was significantly higher after treatment with adenosine ($P = 0.0010$ for 750 µM, $P = 0.0010$ for 1 mM, $P = 0.0108$ for 1.5 mM) (Figure 6 J through P). Uric acid produced severe reductions in LDHA activity, with almost 20% and 30% reduction of relative LDHA activity after treatment with 750 µM and 1 mM uric acid, respectively.

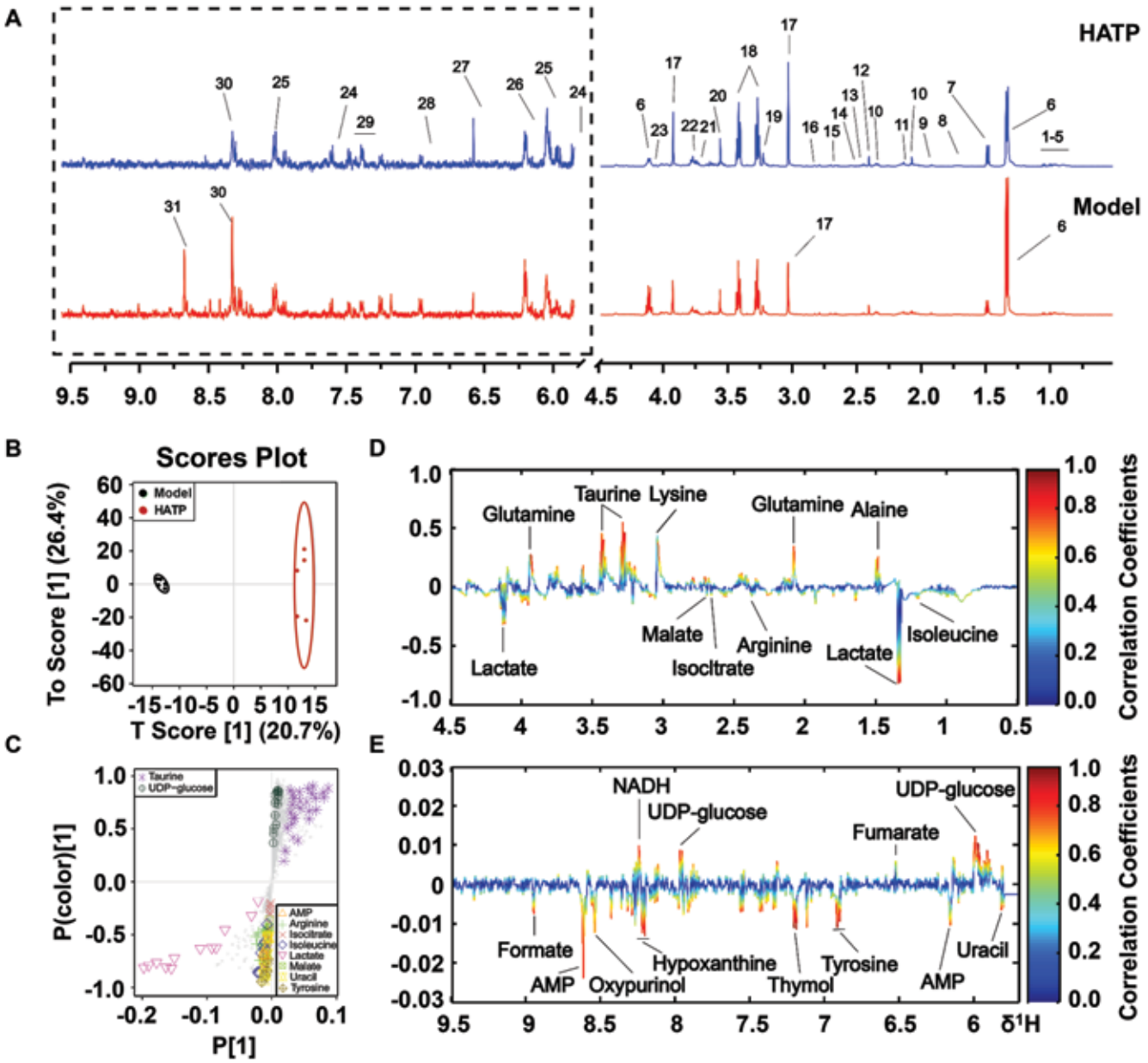

Figure 3. ATP altered intratumoral metabolic profiling. (A) Typical spectra of tumor extracts with assigned metabolites from the Model and HATP groups. (B) Score plots, (C) S-plot, and (D, E) color-coded loading according to orthogonal partial least-squares discriminant analysis of tumor metabolomics profiles in the Model and HATP groups. The color bar corresponds to the weight of the associated variable to distinguish the statistically significant (red) or insignificant (blue) differences. Upward and downward peaks demonstrate relative increases and decreases, respectively, in the metabolites in the HATP group. The assigned metabolites are: 1, leucine; 2, 2-hydroxybutyrate; 3, isoleucine; 4, valine; 5, isobutyrate; 6, lactate; 7, alanine; 8, lysine; 9, arginine; 10, glutamate; 11, methionine; 12, succinate; 13, citrate; 14, isocitrate; 15, malate; 16, glutathione; 17, creatine phosphate; 18, taurine; 19, glucose; 20, glycine; 21, glutamine; 22, ascorbate; 23, myoinositol; 24, uracil; 25, UDP-glucose; 26, AMP; 27, fumarate; 28, tyrosine; 29, phenylalanine; 30, oxypurinol; and 31, formate.

These data suggest that ATP and its metabolite uric acid reduced LDHA activity and thereby suppressed melanoma cell growth.

Effect of ATP on the production of reactive oxygen species and AMPK activation. Impaired glycolysis and pentose phosphate pathway could induce oxidative stress by decreasing NADPH generation[17] and AMPK regulates NADPH homeostasis to promote tumor cell survival during energy stress.[20,36] Therefore, we measured reactive oxygen species and the AMPK activity of B16F10 cells after treatment with ATP for 24 h. The data showed that ATP treatment increased levels of reactive oxygen species in the B16F10 cells (P = 0.0173 for 500 μM, P = 0.0017 for 750 μM, P < 0.0001 for 1 mM, P <0.0001 for 1.5 mM) (Figure 7 A), whereas the levels of phosphorylated AMPK and AMPK were lower in the ATP-treated B16F10 cells than in control cells (Figure 7 B). These results indicate that ATP stimulates the production of reactive oxygen species and impairs AMPK activation.

Discussion

The metabolomic profile of ATP-treated mouse melanoma tumors revealed a dramatic decrease in several metabolites associated with energy metabolism. Tumor cells consume more glucose than do normal cells, and the low levels of glucose in the tumors of ATP-treated mice can be interpreted as decreased glucose absorption due to exogenous ATP.[55] Tumor cells are

Table 1. Identified intratumoral metabolites with peak assignments, chemical shift, fold change, and *P* values

Metabolites	Assignments	Chemical shift (ppm)[a]	log_2(FC)[b]	*P*[c]	
Leucine	δ-CH_3, δ-CH_3, γ-CH	0.95 (d), 0.97 (d), 1.74 (m)	−0.10489	0.1929	
2-Hydroxybutyrate	CH_3	0.95 (t)	−0.18661	0.1219	
Isoleucine	δ-CH_3, γ-CH_3, α-CH	0.96 (t), 1.01 (d), 3.66 (d)	−0.33237	0.0350	*
Valine	γ-CH_3, γ-CH_3, α-CH	0.97 (d), 1.02 (d), 3.40 (d)	−0.25936	0.1075	
Isobutyrate	CH_3	1.04 (d)	−0.1218	0.1883	
Lactate	CH_3, CH	1.32 (d), 4.11 (q)	−0.17003	0.0203	*
Alanine	CH_3, CH	1.48 (t), 3.76 (q)	0.092212	0.1015	
Lysine	δ-CH_2, ε-CH_2	1.72 (m), 3.02 (t)	0.173707	0.2117	
Arginine	β-CH2	1.92 (m)	−0.7768	0.0325	*
Glutamate	β-CH_2, γ-CH_2, α-CH	2.04 (m), 2.33 (m), 3.75 (q)	−0.06359	0.2646	
Glutamine	β-CH_2, γ-CH_2, α-CH	2.11 (m), 2.44 (m), 3.76 (t)	0.254029	0.0895	
Methionine	S-CH_3	2.14 (s)	−0.12789	0.1599	
Succinate	CH_2	2.40 (s)	−0.061	0.2791	
Citrate	1/2CH, 1/2CH	2.53 (d), 2.70 (d)	−0.90449	0.1027	
Isocitrate	γ-CH_2	2.55 (m)	−0.46183	0.0246	*
Malate	CH_2	2.69 (dd)	−1.21795	0.0237	*
Glutathione	SH-CH_2	2.98 (m)	−0.09105	0.3117	
Creatine phosphate	CH_3	3.05 (s)	−0.45991	0.1552	
Taurine	CH_2SO_3	3.26 (t)	0.105762	0.0107	*
Glucose	CH, CH_2, CH_2	3.40-3.55 (m), 3.90 (m), 5.24 (d)	−0.65316	0.1508	
Glycine	CH_2	3.57 (s)	−0.08192	0.1280	
Ascorbate	CH_2	3.76 (d)	0.023485	0.3617	
myo-Inositol	H_5	4.07 (t)	0.146875	0.1318	
Uracil	α-CH, β-CH	5.80 (d), 7.54 (d)	−0.35832	0.0275	*
UDP-glucose	CH, CH, CH	5.97 (d), 5.98 (d), 7.96 (d)	0.182078	0.0331	*
AMP	CH, CH, CH	6.15 (d), 8.27 (s), 8.62 (s)	−1.49925	0.0183	*
Fumarate	CH = CH	6.53 (s)	0.207904	0.1172	
Tyrosine	CH	6.90 (d)	−1.0425	2.6×10^{-5}	†
Phenylalanine	CH = CH	7.32 (m), 7.37 (m), 7.42 (m)	−0.15136	0.1557	
Oxypurinol	CH	8.27 (s)	−0.25302	0.1314	
Formate	H-CO	8.46 (s)	−0.42679	0.2776	

[a]Multiplicity: s, singlet; d, doublet; dd, double doublet; t, triplet; q, quartet; m, multiplet.
[b]Color-coded according to the logarithmic transformation of fold change log_2 (FC) in the HATP group (red, increased; and blue, decreased).
[c]*P* values were calculated by using a parametric Student *t* test (*, $P < 0.05$; †, $P < 0.01$).

known to primarily use glucose to produce lactate, which accumulates in the tumor environment and promotes tumor growth.[13] The reduction of the intermediates citrate, isocitrate, malate, and succinate after ATP treatment may indicate decreased flux toward the tricarboxylic acid cycle (Figure 8). Fumarate, which may be produced by phenylalanine and tyrosine metabolism, was the only intermediate that increased in ATP-treated tumors. Moreover, the depletion of anaplerotic amino acids in ATP-treated tumors suggests entry into the tricarboxylic acid cycle. Excess accumulation of the oncometabolite 2-hydroxyglutarate has been shown to lead to an elevated risk of a range of malignant tumors.[8] The intratumor levels of lactate and AMP were lower and the level of UDP-glucose was higher after ATP treatment. The results indicate that the pathway diverting glucose to lactate was suppressed as a result of reduced LDHA activity, which led to reduced production of lactate and accumulation of UDP-glucose.

In addition to rapid glucose catabolism, many types of cancers are characterized by elevated amino acid levels. Amino acids are a fundamental brick of cell structure that support protein synthesis.[5] Isoleucine is an essential amino acid that can be broken down to generate many metabolites that participate in other metabolic pathways.[37] In cancer growth, isoleucine is consumed in various biosynthetic pathways to supply energy, demonstrating the significance of isoleucine metabolism in tumor therapy.[33] In our current study, the marked reduction of isoleucine after ATP treatment indicates a status of energy deficiency in melanoma-bearing mice. Arginine, a non- or semi-essential amino acid, fulfills various cellular functions, especially in tumor cells with large nutritional needs.[49] For arginine auxotrophic tumors like melanoma, arginine depletion has been considered as a potential treatment for cancer.[47] Our results show a reduction of arginine after ATP treatment, consistent with an earlier report.[57] Tyrosine is one of the 3 major amino acid residues in proteins, and tyrosine phosphorylation may promote tumor growth.[27,51] The lower level of tyrosine in our mouse melanoma model also indicates attenuated tumor growth.

Through activating signal transduction pathways or immune cells, extracellular ATP has been shown to exert an inhibitory effect on many types of cancer.[22] ATP in the tumor microenvironment can provide a stimulatory signal for the innate or adaptive immune responses to tumor cells, thus promoting antitumor immunity.[22] Specifically, ATP in the extracellular environment has a high affinity for phagocytes, promoting the chemotaxis of phagocytes and engulfment of tumor cells.[3] In addition, extracellular ATP can bind to the purinergic receptors

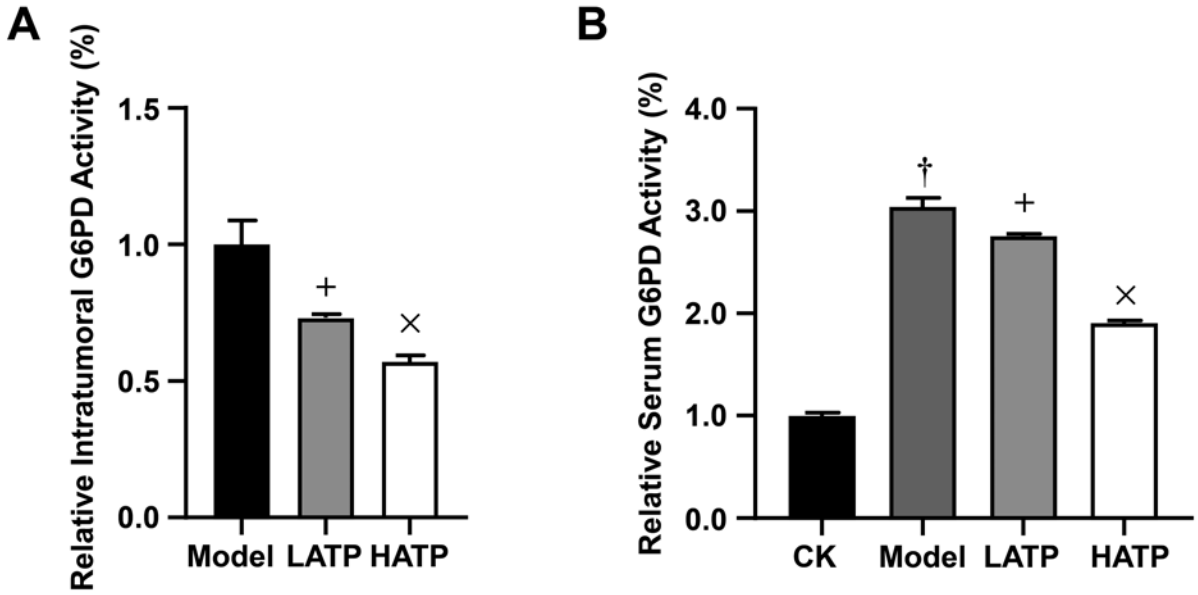

Figure 4. ATP treatment downregulated the glucose-6-phosphate dehydrogenase (G6PD) activity in tumors and serum. (A) Intratumoral G6PD activity in melanoma-bearing mice. (B) Serum G6PD activities in the four groups. Data are shown as mean ± 1 SD (n = 5). *, $P < 0.05$; †, $P < 0.01$ compared with the CK group; +, $P < 0.05$; ×, $P < 0.01$ compared with the Model group.

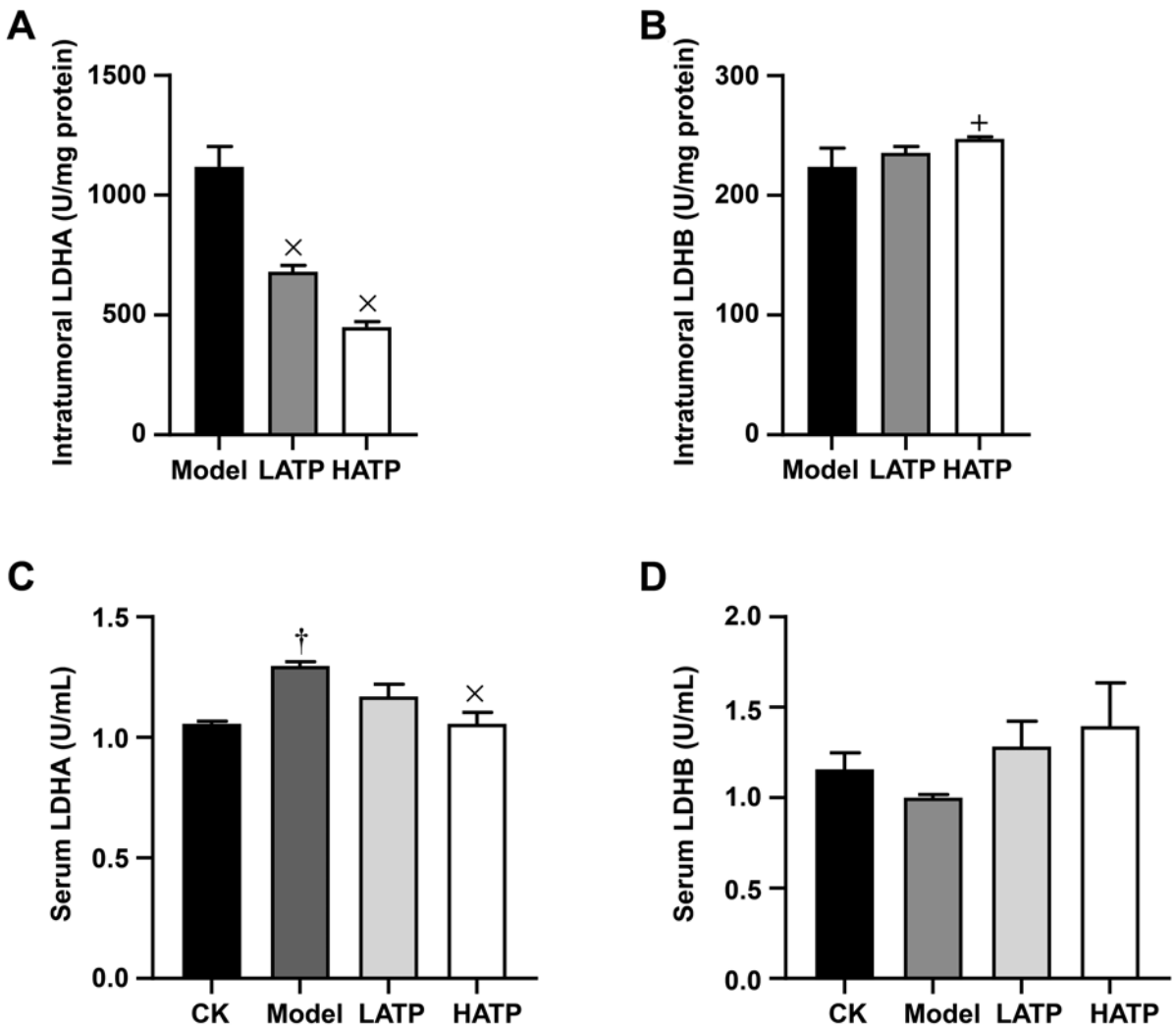

Figure 5. ATP inhibited LDHA activity in tumors and serum. (A) Intratumoral LDHA activity in melanoma-bearing mice. (B) Intratumoral LDHB activities in melanoma-bearing mice. (C) LDHA activity in serum. (D) LDHB activity in serum. Data are shown as mean ± 1 SD ($n = 5$). *, $P < 0.05$; †, $P < 0.01$ compared with the CK group; +, $P < 0.05$; ×,$P < 0.01$ compared with the Model group.

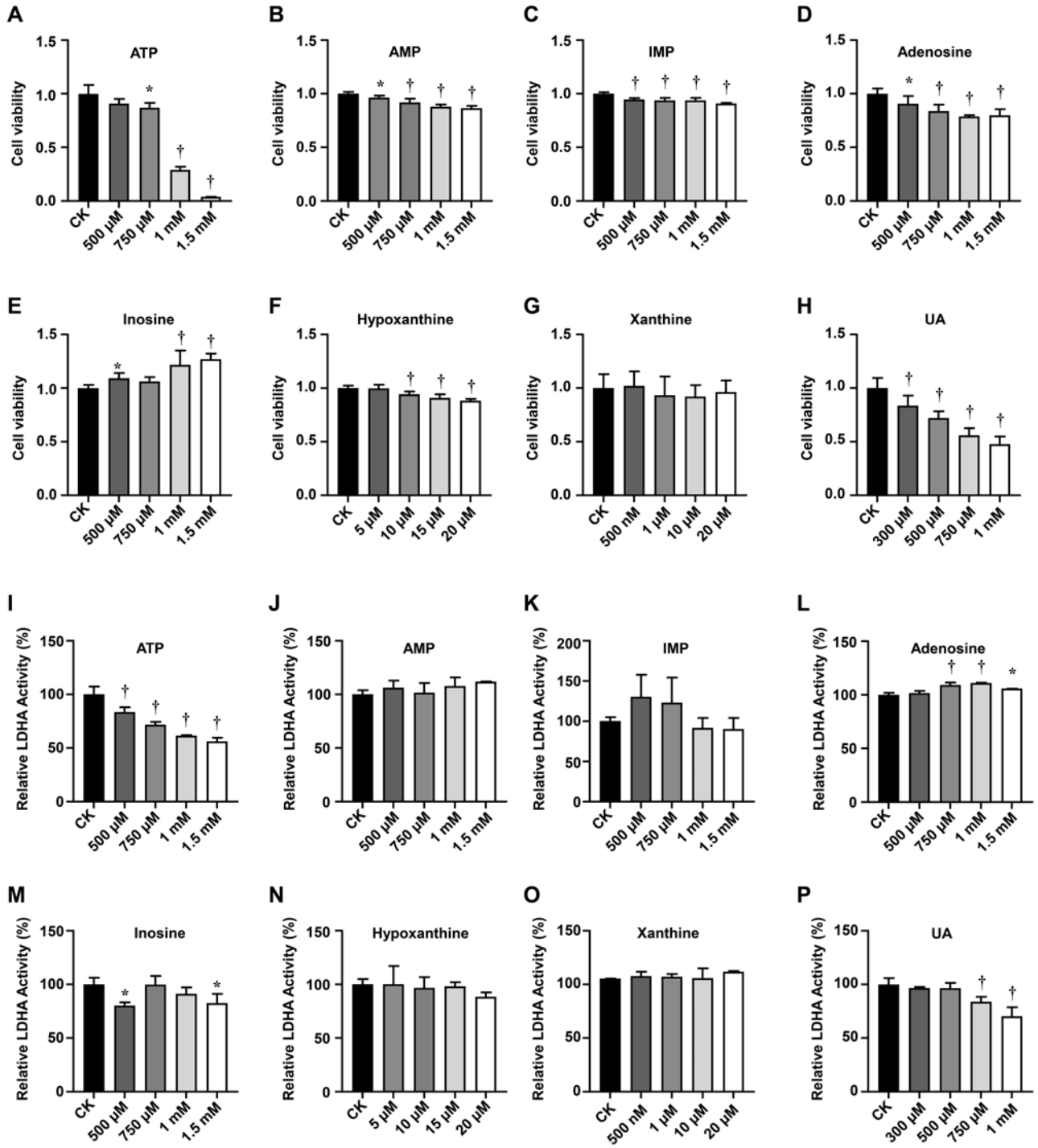

Figure 6. ATP and its metabolites exerted cytotoxicity and inhibited LDHA activity in B16F10 cells. The cell viability of B16F10 cells under treatment with nucleotides, including (A) ATP, (B) AMP, and (C) IMP for 24 h. The cell viability of B16F10 cells under treatments with adenine nucleotide metabolites, including (D) adenosine, (E) inosine, (F) hypoxanthine, (G) xanthine, and (H) uric acid for 24 h. The LDHA activity of B16F10 cells under treatment with nucleotides, including (I) ATP, (J) AMP, and (K) IMP for 24 h. The LDHA activity of B16F10 cells under treatment with adenine nucleotide metabolites, including (L) adenosine, (M) inosine, (N) hypoxanthine, (O) xanthine, and (P) uric acid for 24 h. Data are shown as mean ± 1 SD ($n = 6$). *, $P < 0.05$; †, $P < 0.01$ compared with the CK group.

that are widely expressed on immune cells, including infiltrating dendritic cells, a kind of antigen-presenting cell, therefore playing a pivotal role in attracting and activating immune cells and promoting the efficient presentation of tumor antigens.[10] In the present study, the significant reduction of tumor size and tumor weight further supported the anticancer efficacy of ATP. However, ATP treatment also reduced LDHA activity and did not enhance the immune function of T-cell and B cell subsets. These results indicate a special relationship between ATP and cancer that is related to altered metabolism rather than to activation of T and B cells. In addition, our data showed that ATP and some of its metabolites, especially uric acid, had high cytotoxicity against B16F10 cells and reduced tumor cell proliferation by inhibiting LDHA activity. Uric acid, a powerful antioxidant and

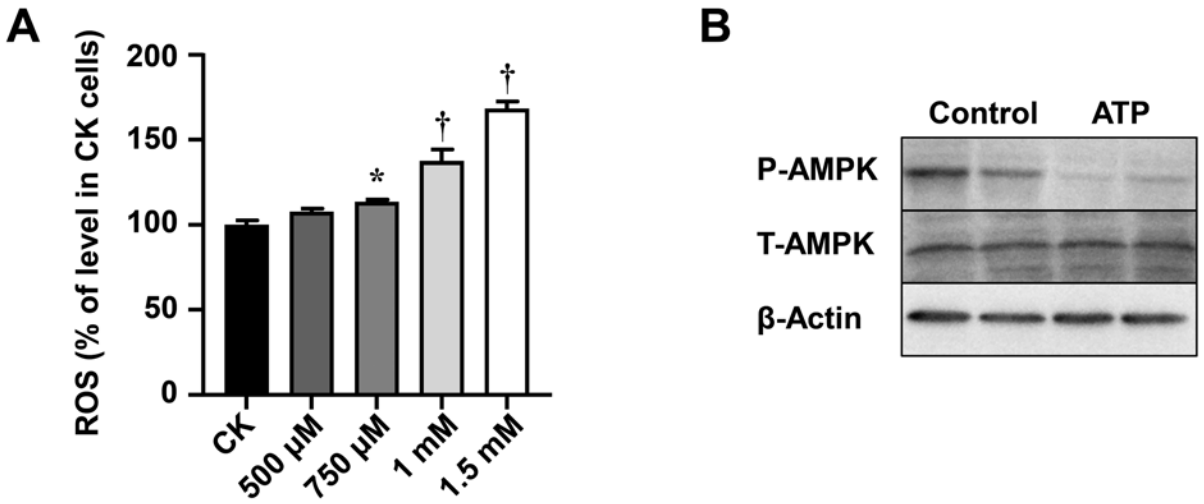

Figure 7. ATP stimulated the production of reactive oxygen species (ROS) and impaired AMPK activation. (A) The level of reactive oxygen species in B16F10 cells under treatment with ATP. (B) The levels of AMPK (T-AMPK) and phosphorylated AMPK (P-AMPK) in B16F10 cells under treatment with ATP. β-actin was used as an internal reference. Data are shown as mean ± 1 SD (n = 6). *, $P < 0.05$; †, $P < 0.01$ compared with the CK group.

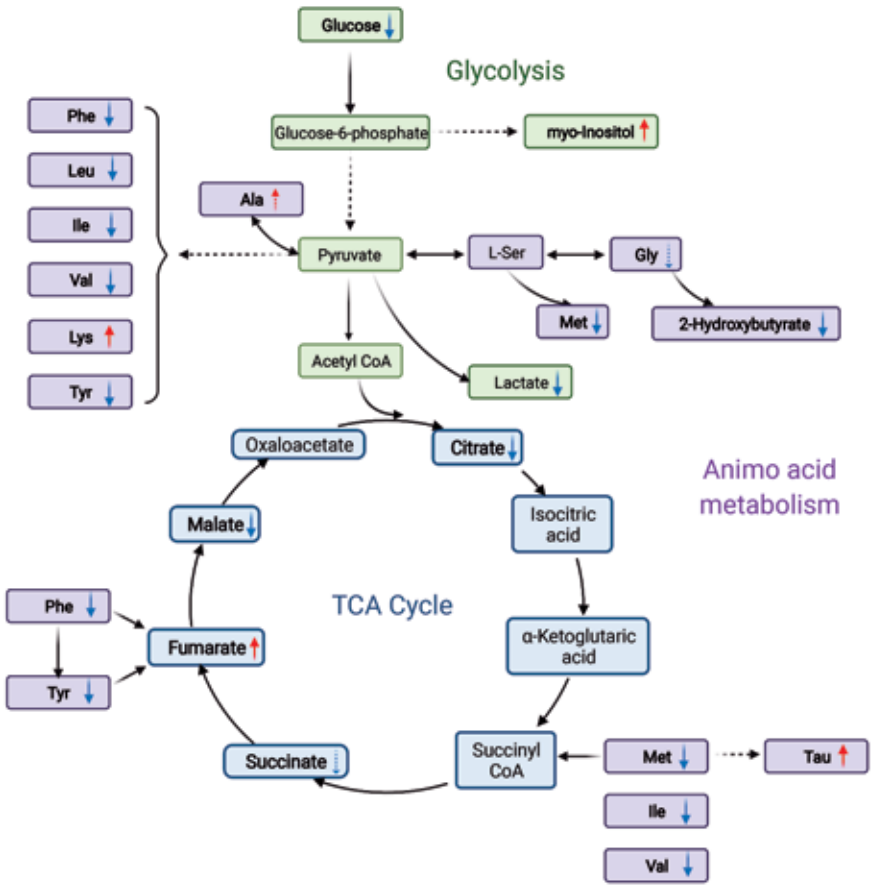

Figure 8. Schematic representation of the main metabolic differences between ATP-treated and untreated tumors. Bold text indicates metabolites whose levels differed between the 2 groups (red, downregulation; yellow, upregulation; dashed lines indicate weak effects). TCA cycle, tricarboxylic acid cycle.

a scavenger of singlet oxygen and radicals, has been recognized as an anticarcinogen in oxidant- and radical-caused cancers.[1] Our findings provide new insights into the anticancer effects of extracellular ATP and uric acid, which synergistically limit tumor cell growth through inhibition of LDHA activity.

Altered cellular metabolism is a hallmark of cancer and is reported to be associated with tumor initiation, progression, and metastasis.[32] Aerobic glycolysis, a common metabolic pathway in cancer cells, diverts glucose to lactate regardless of oxygen availability, promoting biomass synthesis and cell

proliferation.[42] LDHA is crucial in the fermentative portion of aerobic glycolysis and has been investigated extensively in previous antitumor research.[11,46,50] In the present study, ATP effectively suppressed melanoma growth and LDHA activity in tumors and serum. The metabolomic profile of ATP-treated tumors revealed a dramatic reduction in several metabolites associated with energy metabolism. Similar to in vivo results, ATP exhibited cytotoxicity toward B16F10 cells and strong inhibition of LDHA activity. However, various ATP metabolites—including AMP, IMP, adenosine, inosine, hypoxanthine, xanthine, and uric acid—had different effects on cytotoxicity and LDHA activity in melanoma cells. Among these metabolites, uric acid exhibited superior antitumor activity and LDHA inhibitory activity. The results in vivo and in vitro demonstrated that ATP and its metabolites, especially uric acid, reduced LDHA activity, disrupting intratumoral energy metabolism and thus limiting melanoma growth.

In conclusion, our study showed that treatment with ATP alters glucose and amino acid metabolism, causing disorders in intratumoral energy metabolism and restraining melanoma growth. Furthermore, ATP and its metabolite uric acid acted as LDHA inhibitors to disrupt tumor energy metabolism.

References

1. **Ames BN, Cathcart R, Schwiers E, Hochstein P.** 1981. Uric acid provides an antioxidant defense in humans against oxidant-and radical-caused aging and cancer: a hypothesis. Proc Natl Acad Sci USA **78:**6858–6862. https://doi.org/10.1073/pnas.78.11.6858.
2. **Beckonert O, Keun HC, Ebbels TM, Bundy J, Holmes E, Lindon JC, Nicholson JK.** 2007. Metabolic profiling, metabolomic and metabonomic procedures for NMR spectroscopy of urine, plasma, serum and tissue extracts. Nat Protoc **2:**2692–2703. https://doi.org/10.1038/nprot.2007.376.
3. **Boyd-Tressler A, Penuela S, Laird DW, Dubyak GR**. 2014. Chemotherapeutic drugs induce ATP release via caspase-gated pannexin-1 channels and a caspase/pannexin-1-independent mechanism. J Biol Chem **289**:27246-27263. https://doi.org/10.1074/jbc.m114.590240.
4. **Burnstock G.** 2017. Purinergic signalling: therapeutic developments. Front Pharmacol **8:**661. https://doi.org/10.3389/fphar.2017.00661.
5. **Cao Y, Liu S, Liu K, Abbasi IHR, Cai C, Yao J.** 2019. Molecular mechanisms relating to amino acid regulation of protein synthesis. Nutr Res Rev **32:**183–191. https://doi.org/10.1017/S0954422419000052.
6. **Chiarella AM, Ryu YK, Manji GA, Rustgi AK.** 2021. Extracellular ATP and Adenosine in Cancer Pathogenesis and Treatment. Trends Cancer **7:**731–750. https://doi.org/10.1016/j.trecan.2021.04.008.
7. **Coyle T, Levante S, Shetler M, Winfield J.** 1994. In vitro and in vivo cytotoxicity of gossypol against central nervous system tumor cell lines. J Neurooncol **19:**25–35. https://doi.org/10.1007/BF01051046.
8. **Dang L, White DW, Gross S, Bittinger MA, Driggers EM, Fantin VR, Jang HG, Jin SF, Keenan MC, Marks KM, Yen KE, Ward PS, Prins RM, Liau LM, Bennett BD, Rabinowitz JD, Cantley LC, Thompson CB, Heiden MV, Su SM.** 2010. Cancer-associated IDH1 mutations produce 2-hydroxyglutarate. Cancer Res **70:**3. https://doi.org/10.1038/nature08617
9. **Di Virgilio F, Adinolfi E.** 2017. Extracellular purines, purinergic receptors and tumor growth. Oncogene **36:**293–303. https://doi.org/10.1038/onc.2016.206.
10. **Di Virgilio F, Sarti AC, Falzoni S, De Marchi E, Adinolfi E.** 2018. Extracellular ATP and P2 purinergic signalling in the tumour microenvironment. Nat Rev Cancer **18:**601–618. https://doi.org/10.1038/s41568-018-0037-0.
11. **Fantin VR, St-Pierre J, Leder P.** 2006. Attenuation of LDH-A expression uncovers a link between glycolysis, mitochondrial physiology, and tumor maintenance. Cancer Cell **9:**425–434. https://doi.org/10.1016/j.ccr.2006.04.023.
12. **Farabegoli F, Vettraino M, Manerba M, Fiume L, Roberti M, Di Stefano G.** 2012. Galloflavin, a new lactate dehydrogenase inhibitor, induces the death of human breast cancer cells with different glycolytic attitude by affecting distinct signaling pathways. Eur J Pharm Sci **47:**729–738. https://doi.org/10.1016/j.ejps.2012.08.012.
13. **Feng Y, Xiong Y, Qiao T, Li X, Jia L, Han Y.** 2018. Lactate dehydrogenase A: A key player in carcinogenesis and potential target in cancer therapy. Cancer Med **7:**6124–6136. https://doi.org/10.1002/cam4.1820.
14. **Finck SJ, Giuliano A, Morton D.** 1983. LDH and melanoma. Cancer **51:**840–843. https://doi.org/10.1002/1097-0142(19830301)51:5<840::AID-CNCR2820510516>3.0.CO;2-7.
15. **Granchi C, Roy S, De Simone A, Salvetti I, Tuccinardi T, Martinelli A, Macchia M, Lanza M, Betti L, Giannaccini G.** 2011. N-Hydroxyindole-based inhibitors of lactate dehydrogenase against cancer cell proliferation. Eur J Med Chem **46:**5398–5407. https://doi.org/10.1016/j.ejmech.2011.08.046.
16. **Guarecuco R, Williams RT, Baudrier L, La K, Passarelli MC, Ekizoglu N, Mestanoglu M, Alwaseem H, Rostandy B, Fidelin J, Garcia-Bermudez J, Molina H, Birsoy K.** 2020. Dietary thiamine influences L-asparaginase sensitivity in a subset of leukemia cells. Sci Adv **6:**eabc7120. https://doi.org/10.1126/sciadv.abc7120.
17. **Honeychurch J, Alduaij W, Azizyan M, Cheadle EJ, Pelicano H, Ivanov A, Huang P, Cragg MS, Illidge TM.** 2012. Antibody-induced nonapoptotic cell death in human lymphoma and leukemia cells is mediated through a novel reactive oxygen species-dependent pathway. Blood **119:**3523–3533. https://doi.org/10.1182/blood-2011-12-395541.
18. **Hu J, Locasale JW, Bielas JH, O'Sullivan J, Sheahan K, Cantley LC, Vander Heiden MG, Vitkup D.** 2013. Heterogeneity of tumor-induced gene expression changes in the human metabolic network. Nat Biotechnol **31:**522–529. https://doi.org/10.1038/nbt.2530.
19. **Jarak I, Carrola J, Barros AS, Gil AM, Pereira Md L, Corvo ML, Duarte IF.** 2017. From the cover: metabolism modulation in different organs by silver nanoparticles: an NMR metabolomics study of a mouse model. Toxicol Sci **159:**422–435. https://doi.org/10.1093/toxsci/kfx142.
20. **Jeon S-M, Chandel NS, Hay N.** 2012. AMPK regulates NADPH homeostasis to promote tumour cell survival during energy stress. Nature **485:**661–665. https://doi.org/10.1038/nature11066.
21. **Jurisic V, Radenkovic S, Konjevic G**. 2015. The actual role of LDH as tumor marker, biochemical and clinical aspects. In: Scatena R, editor. Advances in Cancer Biomarkers. Adv Exp Med Biol **867**: 115–124. https://doi.org/10.1007/978-94-017-7215-0_8
22. **Kepp O, Loos F, Liu P, Kroemer G.** 2017. Extracellular nucleosides and nucleotides as immunomodulators. Immunol Rev **280:**83–92. https://doi.org/10.1111/imr.12571.
23. **Kim E-Y, Choi H-J, Park M-J, Jung Y-S, Lee S-O, Kim K-J, Choi J-H, Chung T-W, Ha K-T.** 2016. Myristica fragrans suppresses tumor growth and metabolism by inhibiting lactate dehydrogenase A. Am J Chin Med **44:**1063–1079. https://doi.org/10.1142/S0192415X16500592.
24. **Kuk D, Shoushtari AN, Barker CA, Panageas KS, Munhoz RR, Momtaz P, Ariyan CE, Brady MS, Coit DG, Bogatch K.** 2016. Prognosis of mucosal, uveal, acral, nonacral cutaneous, and unknown primary melanoma from the time of first metastasis. Oncologist **21:**848–854. https://doi.org/10.1634/theoncologist.2015-0522.
25. **Larkin J, Minor D, D'Angelo S, Neyns B, Smylie M, Miller WH Jr, Gutzmer R, Linette G, Chmielowski B, Lao CD.** 2018. Overall survival in patients with advanced melanoma who received nivolumab versus investigator's choice chemotherapy in CheckMate 037: a randomized, controlled, open-label phase III trial. J Clin Oncol **36:**383–390. https://doi.org/10.1200/JCO.2016.71.8023.
26. **Le A, Cooper CR, Gouw AM, Dinavahi R, Maitra A, Deck LM, Royer RE, Vander Jagt DL, Semenza GL, Dang CV.** 2010. Inhibition of lactate dehydrogenase A induces oxidative stress and inhibits tumor progression. Proc Natl Acad Sci USA **107:**2037–2042. https://doi.org/10.1073/pnas.0914433107.
27. **Liu R, Li W, Tao B, Wang X, Yang Z, Zhang Y, Wang C, Liu R, Gao H, Liang J.** 2019. Tyrosine phosphorylation activates 6-phosphogluconate dehydrogenase and promotes tumor growth

and radiation resistance. Nat Commun **10:**991–1004. https://doi.org/10.1038/s41467-019-08921-8.

28. **Lorenzi PL, Reinhold WC, Rudelius M, Gunsior M, Shankavaram U, Bussey KJ, Scherf U, Eichler GS, Martin SE, Chin K, Gray JW, Kohn EC, Horak ID, Von Hoff DD, Raffeld M, Goldsmith PK, Caplen NJ, Weinstein JN.** 2006. Asparagine synthetase as a causal, predictive biomarker for L-asparaginase activity in ovarian cancer cells. Mol Cancer Ther **5:**2613–2623. https://doi.org/10.1158/1535-7163.MCT-06-0447.
29. **Luke JJ, Flaherty KT, Ribas A, Long GV.** 2017. Targeted agents and immunotherapies: optimizing outcomes in melanoma. Nat Rev Clin Oncol **14:**463–482. https://doi.org/10.1038/nrclinonc.2017.43.
30. **Maecker HT, McCoy JP, Nussenblatt R.** 2012. Standardizing immunophenotyping for the human immunology project. Nat Rev Immunol **12:**191–200. https://doi.org/10.1038/nri3158.
31. **Miao P, Sheng S, Sun X, Liu J, Huang G.** 2013. Lactate dehydrogenase A in cancer: a promising target for diagnosis and therapy. IUBMB Life **65:**904–910. https://doi.org/10.1002/iub.1216.
32. **Pavlova NN, Thompson CB.** 2016. The emerging hallmarks of cancer metabolism. Cell Metab **23:**27–47. https://doi.org/10.1016/j.cmet.2015.12.006.
33. **Peng H, Wang Y, Luo W.** 2020. Multifaceted role of branched-chain amino acid metabolism in cancer. Oncogene **39:**6747–6756. https://doi.org/10.1038/s41388-020-01480-z.
34. **Percie du Sert N, Hurst V, Ahluwalia A, Alam S, Avey MT, Baker M, Browne WJ, Clark A, Cuthill IC, Dirnagl U, Emerson M, Garner P, Holgate ST, Howells DW, Karp NA, Lazic SE, Lidster K, MacCallum CJ, Macleod M, Pearl EJ, Petersen OH, Rawle F, Reynolds P, Rooney K, Sena ES, Silberberg SD, Steckler T, Würbel H.** 2020. The ARRIVE guidelines 2.0: Updated guidelines for reporting animal research. PLOS Biol **18**:e3000410. https://doi.org/10.1371/journal.pbio.3000410.
35. **R Core Team.** [Internet]. 2014. R: A language and environment for statistical computing. R Foundation for Statistical Computing, Vienna, Austria. Available at: http://www.R-project.org/.
36. **Ren Y, Shen H-M.** 2019. Critical role of AMPK in redox regulation under glucose starvation. Redox Biol **25:**101154. https://doi.org/10.1016/j.redox.2019.101154.
37. **Sivanand S, Vander Heiden MG.** 2020. Emerging roles for branched-chain amino acid metabolism in cancer. Cancer Cell **37:**147–156. https://doi.org/10.1016/j.ccell.2019.12.011.
38. **Stefan E, Hofmann S, Tampé R.** 2020. A single power stroke by ATP binding drives substrate translocation in a heterodimeric ABC transporter. eLife **9:**e55943. https://doi.org/10.7554/eLife.55943.
39. **Suarez RK.** 2012. Energy and metabolism. Compr Physiol **2:**2527–2540. https://doi.org/10.1002/cphy.c110009.
40. **Sung H, Ferlay J, Siegel RL, Laversanne M, Soerjomataram I, Jemal A, Bray F.** 2021. Global cancer statistics 2020: GLOBOCAN estimates of incidence and mortality worldwide for 36 cancers in 185 countries. CA Cancer J Clin **71:**209–249. https://doi.org/10.3322/caac.21660.
41. **Tamajusuku AS, Villodre ES, Paulus R, Coutinho-Silva R, Battasstini AM, Wink MR, Lenz G.** 2010. Characterization of ATP-induced cell death in the GL261 mouse glioma. J Cell Biochem **109:**983–991. https://doi.org/10.1002/jcb.22478.
42. **Vander Heiden MG, Cantley LC, Thompson CB.** 2009. Understanding the Warburg effect: the metabolic requirements of cell proliferation. Science **324:**1029–1033. https://doi.org/10.1126/science.1160809.
43. **Vazquez-Lombardi R, Loetsch C, Zinkl D, Jackson J, Schofield P, Deenick EK, King C, Phan TG, Webster KE, Sprent J, Christ D.** 2017. Potent antitumour activity of interleukin-2-Fc fusion proteins requires Fc-mediated depletion of regulatory T-cells. Nat Commun **8:**15373. https://doi.org/10.1038/ncomms15373.
44. **Vultaggio-Poma V, Sarti AC, Di Virgilio F.** 2020. Extracellular ATP: a feasible target for cancer therapy. Cells **9:**2496. https://doi.org/10.3390/cells9112496.
45. **Wang X, Hu M, Feng J, Liu M, Hu JZ.** 2014. 1 H NMR metabolomics study of metastatic melanoma in C57BL/6J mouse spleen. Metabolomics **10:**1129–1144. https://doi.org/10.1007/s11306-014-0652-z.
46. **Wang Z-Y, Loo TY, Shen J-G, Wang N, Wang D-M, Yang D-P, Mo S-L, Guan X-Y, Chen J-P.** 2012. LDH-A silencing suppresses breast cancer tumorigenicity through induction of oxidative stress mediated mitochondrial pathway apoptosis. Breast Cancer Res Treat **131:**791–800. https://doi.org/10.1007/s10549-011-1466-6.
47. **Wettersten HI, Aboud OA, Lara PN, Weiss RH.** 2017. Metabolic reprogramming in clear cell renal cell carcinoma. Nat Rev Nephrol **13:**410–419. https://doi.org/10.1038/nrneph.2017.59.
48. **White N, Knight GE, Butler PE, Burnstock G.** 2009. An in vivo model of melanoma: treatment with ATP. Purinergic Signal **5:**327–333. https://doi.org/10.1007/s11302-009-9156-0.
49. **Yang J-S, Wang C-C, Qiu J-D, Ren B, You L.** 2021. Arginine metabolism: a potential target in pancreatic cancer therapy. Chin Med J (Engl) **134:**28–37. https://doi.org/10.1097/CM9.0000000000001216.
50. **Yeung C, Gibson AE, Issaq SH, Oshima N, Baumgart JT, Edessa LD, Rai G, Urban DJ, Johnson MS, Benavides GA.** 2019. Targeting glycolysis through inhibition of lactate dehydrogenase impairs tumor growth in preclinical models of Ewing sarcoma. Cancer Res **79:**5060–5073. https://doi.org/10.1158/0008-5472.CAN-19-0217.
51. **Yu J-S.** 2019. From discovery of tyrosine phosphorylation to targeted cancer therapies: the 2018 Tang Prize in Biopharmaceutical Science. Biomed J **42:**80–83. https://doi.org/10.1016/j.bj.2019.03.004.
52. **Yun J, Rago C, Cheong I, Pagliarini R, Angenendt P, Rajagopalan H, Schmidt K, Willson JKV, Markowitz S, Zhou SB, Diaz LA, Velculescu VE, Lengauer C, Kinzler KW, Vogelstein B, Papadopoulos N.** 2009. Glucose Deprivation Contributes to the Development of KRAS Pathway Mutations in Tumor Cells. Science **325:**1555–1559. https://doi.org/10.1126/science.1174229.
53. **Zawistowski JS, Bevill SM, Goulet DR, Stuhlmiller TJ, Beltran AS, Olivares-Quintero JF, Singh D, Sciaky N, Parker JS, Rashid NU, Chen X, Duncan JS, Whittle MC, Angus SP, Velarde SH, Golitz BT, He X, Santos C, Darr DB, Gallagher K, Graves LM, Perou CM, Carey LA, Earp HS, Johnson GL.** 2017. Enhancer Remodeling during Adaptive Bypass to MEK Inhibition Is Attenuated by Pharmacologic Targeting of the P-TEFb Complex. Cancer Discov **7**:302–321. https://doi.org/10.1158/2159-8290.CD-16-0653.
54. **Ždralević M, Brand A, Di Ianni L, Dettmer K, Reinders J, Singer K, Peter K, Schnell A, Bruss C, Decking S-M, Koehl G, Felipe-Abrio B, Durivault J, Bayer P, Evangelista M, O'Brien T, Oefner PJ, Renner K, Pouysségur J, Kreutz M.** 2018. Double genetic disruption of lactate dehydrogenases A and B is required to ablate the "Warburg effect" restricting tumor growth to oxidative metabolism. J Biol Chem **293:**15947–15961. https://doi.org/10.1074/jbc.RA118.004180.
55. **Zhao Y, Cheng R, Zhao Y, Ge W, Yang Y, Ding Z, Xu X, Wang Z, Wu Z, Zhang J.** 2021. Type 2 diabetic mice enter a state of spontaneous hibernation-like suspended animation following accumulation of uric acid. J Biol Chem **297:**101166. https://doi.org/10.1016/j.jbc.2021.101166.
56. **Zhou Z, Deng H, Yang W, Wang Z, Lin L, Munasinghe J, Jacobson O, Liu Y, Tang L, Ni Q, Kang F, Liu Y, Niu G, Bai R, Qian C, Song J, Chen X.** 2020. Early stratification of radiotherapy response by activatable inflammation magnetic resonance imaging. Nat Commun **11**:3032. https://doi.org/10.1038/s41467-020-16771-y.
57. **Zou S, Wang X, Liu P, Ke C, Xu S.** 2019. Arginine metabolism and deprivation in cancer therapy. Biomed Pharmacother **118:**109210. https://doi.org/10.1016/j.biopha.2019.109210.